IC/IR/2005/019
INTERNAL REPORT
(Limited Distribution)

United Nations Educational Scientific and Cultural Organization
and
International Atomic Energy Agency

THE ABDUS SALAM INTERNATIONAL CENTRE FOR THEORETICAL PHYSICS

THERMAL BEHAVIOUR OF A SOLAR AIR HEATER WITH A COMPOUND PARABOLIC CONCENTRATOR

Réné Tchinda[1]
IUT FOTSO VICTOR, University of Dschang,
P.O. Box, 134 Bandjoun, Cameroon
and
The Abdus Salam International Centre for Theoretical Physics, Trieste, Italy.

Abstract

A mathematical model for computing the thermal performance of an air heater with a truncated compound parabolic concentrator having a flat one-sided absorber is presented. A computed code that employs an iterative solution procedure is constructed to solve the governing energy equations and to estimate the performance parameters of the collector. The effects of the air mass flow rate, the wind speed and the collector length on the thermal performance of the present air heater are investigated. Prediction for the performance of the solar heater also exhibits reasonable agreement with experimental data with an average error of 7%.

MIRAMARE – TRIESTE

November 2005

[1] Regular Associate of ICTP.

1- Introduction

Simulation models are important design tools and are useful for predicting the collector's experimental performance. In any solar energy application, it would be desirable to analyse theoretically any given system as extensively as possible before embarking the construction of one for installation. Rabl (1976), Hsieh (1981), Prapas et al. (1987), Norton et al. (1989), Eames and Norton (1993), and Oommen and Jayaraman (2001) analysed non evacuated CPC cavities with flat or cylindrical absorber. The thermal analyses of such collectors have been well documented (Tchinda et al. 1998, Fraidenraich et al. 1999, Tchinda 2003).

However, a close examination of the papers revealed that the case of a cylindrical absorber is of particular interest because standard piping and evacuated tubes are commonplace receiver elements, and because the cylindrical shape reduces thermal losses through the back of the collector. Other CPC configurations like non-evacuated stationary CPC solar collector with flat bifacial absorber (Tripanagnostopoulos et al. 2000), CPC augmented with a reverse flat plate absorber (Eames et al. 2001), asymmetric compound parabolic concentrator (Fang et al. 2003, Adsten et al. 2004, Mallick et al. 2004) have been proposed. Papers reporting thermal analysis of the CPC with flat one-side absorber are rarely found, and those published are devoted to the effect of truncation on optical, thermal losses and collectible energy (Carvalho et al. 1985), or to increase the electrical energy output (Gordon 1988). Recently, Pramuang and Exell (2005) reported the results of an experimental study in which the method of Chungpaibulpatana and Excell is used to determine the collector parameters of a solar flat plate collector with a CPC for heating air.

The purpose of this paper is to quantify the heat transfer within compound parabolic concentrating solar energy collectors with flat one-sided absorber. A mathematical model analysing the collector thermal performance is introduced and examined by using a constructed computer code that used an iterative procedure.

2- Structure of CPC and Mathematical modeling

The CPC is capable of accepting solar radiation for long periods each day without diurnal tracking of the sun. It also has the advantage of concentrating the diffuse radiation, which is not possible using an imaging collector (Pramuang and Exell 2005). The two dimensional CPC collector with a flat absorber is the one studied experimentally by Pramuang and Exell (2005). The principal dimensions for the CPC collector used are labelled in figure 1 in both cross section figure 1-a and side view figure 1-b.

In order to simplify the analysis, the following main assumptions are made:

A-1: It is assumed that the CPC is ideal and free from fabrication errors.

A-2: Any beam of radiation incident within the acceptance angle θ_a, with the help of the parabolic reflector can reach the receiver. The concentration ratio used in this work is defined on a geometrical basis and is expressed in terms of the total receiver area ($C_a=1/\sin(\theta_a)=A_C/A_P$) (Hsieh 1981, Carvalho et al. 1985).

A-3: The reflection of radiation from the parabolic reflector is accounted for by the apparent reflectance $\rho_m^{<n>}$, with <n>=0.5+0.07C_a for a CPC with flat plate absorber (Rabl et al. 1979, Tchinda 2003).

A-4 The direction of the beam radiation incident on various components in the collector can be found though geometry. Any reflection from these components, particularly multireflections from the parabolic reflector, will cause a reorientation of rays to the effect that the ray's reflection pattern becomes exceedingly difficult to follow without reliance on a detailed ray tracing. To facilitate analysis these reflections are treated as diffuse and their energy accounted for in terms of diffuse reflectivities (Hsieh 1981, Tchinda 2003). The succeeding absorption and transmission processes inside CPC are diffusive and are accounted for in terms of diffuse properties. The solar and infrared energy exchanges in the collector are treated separately using pertinent radiative properties in the spectrum.

A-5 Physical and optical properties of materials are assumed to be independent of temperature.

A-6 The concentrator does not produce an image of the light source, hence it is called non-imaging concentrators.

Figure 1-c illustrates the electric analogy circuit for the CPC collector. Applying heat balances in a suitable way, the following set of partial differential equations can be derived:

For cover

$$M_c C_{pc} \frac{\partial T_c}{\partial t} = q_c(t) + h_{Rp}(T_p - T_c) + h_{p/c}(T_p - T_c) - h_{Rs}(T_c - T_s) - h_{c/a}(T_c - T_b) \quad (1)$$

with t>0.

For flate absorber

$$M_p C_{pp} \frac{\partial T_p}{\partial t} = q_p(t) - h_{Rp}(T_p - T_c) - h_{p/c}(T_p - T_c) - q_u(t) \quad (2)$$

with t>0.

For fluid

$$\rho_f e_f C_{pf} \frac{\partial T_f}{\partial t} = q_u(t) - \frac{\dot{m} C_{pf}}{l_p} \frac{\partial T_f}{\partial x} - U_0 (T_f - T_b) \quad (3)$$

with t>0 and 0<x<L.

In equations (1) and (2), $q_c(t)$ and $q_p(t)$ have been expressed using the Hsieh's theory (Tchinda, 2003), as:

$$q_c(t) = I(t) \left[\overline{\alpha}_c + \overline{\alpha}_c \overline{\tau}_c \overline{\rho}_p \rho_m^{2\langle n \rangle} \right] \frac{A_c}{A_p} \quad (4)$$

$$q_p(t) = I(t)\, \overline{\tau}_c \rho_m^{\langle n \rangle} P \left[\overline{\alpha}_p + \overline{\alpha}_p \overline{\rho}_p \overline{\rho}_c \frac{A_p}{A_c} \right] \frac{A_c}{A_p} \quad (5)$$

P is the gap loss factor, which is equal to $1-g/l_p$ (Rabl et al. 1979), where g is the gap thickness. $A_c=W*L$ and $A_p=l_p*L$

At any point x, the fluid temperature (T_f) is related to the useful energy q_u (see equations (2) and (3)) and the absorber temperature (T_p) by the following expression:

$$q_u = U_f (T_p - T_f) \quad (6)$$

The factor U_f is the convective heat transfer coefficient between heat transfer fluid and the walls of the absorber is calculated from the relationship:

$$U_f = \frac{N_{uf} \lambda_f}{D_H} \quad (7)$$

where the Nusselt number N_u and the hydraulic diameter D_H are given in the Appendix.

Since the absorptance of the cover and the thermal capacities of the components of the collector are small, we neglect them. However, the functioning of the collector remains variable with time because it depends on the unsteady solar intensity. Eliminating T_c and T_p from the simplified equations obtained, one gets:

$$C_{pf} \dot{m} \frac{dT_f}{dx} = l_p \left[S_p - U_L (T_f - T_b) \right] F' \quad (8)$$

with

$$S_p = I(t)\ \overline{\tau}_c \rho_m^{\langle n \rangle} P \left[\overline{\alpha}_p + \overline{\alpha}_p \overline{\rho}_p \overline{\rho}_c \frac{A_p}{A_c} \right] \frac{A_c}{A_p} + \frac{(h_{Rp} + h_{p/c}) \left(I(t) \left[\overline{\alpha}_c + \overline{\alpha}_c \overline{\tau}_c \overline{\rho}_p \rho_m^{2\langle n \rangle} \right] \frac{A_c}{A_p} \right)}{h_{Rp} + h_{p/c} + h_{Rs} + h_{c/a}} - \frac{(h_{Rp} + h_{p/c}) \Delta T\ h_{Rs}}{h_{Rp} + h_{p/c} + h_{Rs} + h_{c/a}} \quad (9)$$

$$U_L = \frac{(h_{Rp}+h_{p/c}+h_{Rs}+h_{c/a})(U_0 U_f + U_0 h_{Rp} + U_0 h_{p/c} + h_{Rp} U_f + h_{p/c} U_f) + (U_0 - U_f)(h_{Rp}+h_{p/c})^2}{(h_{Rp}+h_{p/c}+h_{Rs}+h_{c/a})U_f} \quad (10)$$

$$F' = \frac{U_f (h_{Rp} + h_{p/c} + h_{c/a} + h_{Rs})}{(h_{Rp} + h_{p/c} + h_{c/a} + h_{Rs})(h_{Rp} + h_{p/c} + U_f) - (h_{Rp} + h_{p/c})^2} \quad (11)$$

To evaluate the collector's performance, it is necessary to estimate the overall loss coefficient U_L, the collector efficiency factor F' and the internal heat transfer coefficients. The relations about the various heat transfer coefficients determined are presented in the Appendix.

Assuming that the overall heat loss coefficient U_L and the collector efficiency factor are temperature independent in position, the efficiency is found to be:

$$\eta_{inst} = \frac{Q_u}{A_C I(t)} \quad (12)$$

where the useful thermal power Q_u extracted from the CPC collector is calculated from the relationship:

$$Q_u = F_R A_r \{S_p - U_L (T_{fe}(0,t) - T_b(t))\} \quad (13)$$

F_R is a removal factor, it is given by:

$$F_R = \frac{C_{pf}\dot{m}}{l_p L U_L}\left(1 - e^{\left(\frac{-l_p L F'_4 U_L}{C_{pf}\dot{m}}\right)}\right) \quad (14)$$

Using equations (12) and (13), η_{insj} becomes:

$$\eta_{inst} = (\eta_0 + F_A) F_R - \frac{U_L}{C_a I(t)} F_R (T_{fe}(0,t) - T_b(t)) \quad (15)$$

where the optical efficiency is given:

$$\eta_0 = \overline{\tau}_c \rho_m^n \overline{\alpha}_p P \left(1 + \overline{\rho}_p \rho_c \frac{l_p}{2W}\right) \quad (16\text{-a})$$

According to Rabl et al. (1980) and to Pramuang and Exell (2005), the optical efficiency is given by:

$$\eta_{01} = \overline{\tau}_c \rho_m^{\langle n \rangle} \overline{\alpha}_p \quad (16\text{-b})$$

The optical efficiency determined from direct measurements (see Pramuang and Exell 2005) of the optical properties of the materials listed in table 1 using equations (16-a and b) have values $\eta_0 \approx 0.72$ and $\eta_{01} \approx 0.75$, respectively. However the result of Pramuang and Exell (2005) obtained using equation (16-b) is different. The difference is due to the fact that in the numerical calculation of Pramuang and Exell (2005), the number of reflections is computed

using the relation <n>=1+0.07C_a which is a relation used for CPC with tubular absorber (Rabl et al. 1979). Analytical results of equation (16-a) agree with the optical efficiency found by direct measurements (η_0=0.67, see Pramuang and Exell 2005) with an error of 7%. Comparing equations (16-a) and (16-b), the ratio gives:

$$\frac{\eta_0}{\eta_{01}} = P\left(1 + \overline{\rho}_p \rho_c \frac{l_p}{2W}\right) < 1 \tag{17}$$

An examination of this equation, when P→1 (g→0, corresponding to a case where reflector touches receiver) shows that equation (16-a) agrees with (16-b) with an average error of 1%. In many solar thermal applications, however, it is necessary to have g≠0 (P<1), because a gap between the reflector and the absorber is needed to reduce conductive heat losses. The above result shows that a gap between the reflector and the absorber causes optical losses, but a compromise between optical and thermal performance must be made.

In equation (15) F_A is named the enclosure absorption factor (Tchinda 2003). It is given by the relationship:

$$F_A = \frac{(h_{Rp} + h_{p/c})}{(h_{Rp} + h_{p/c} + h_{c/a} + h_{Rs})}\left\{\overline{\alpha}_c + \overline{\alpha}_c \overline{\tau}_c \overline{\rho}_p \rho_m^{2\langle n\rangle} - \frac{\Delta T\ h_{Rs}}{I(t)\ C_a}\right\} \tag{18}$$

The performance of the system over a period of a day is computed as the daily average efficiency:

$$\eta = \frac{\int_{t_r}^{t_s} \dot{m} C_{pf} (T_{f0}(L,t) - T_{fe}(0,t) dt}{A_C \int_{t_r}^{t_s} I(t) dt} \tag{19}$$

where t_r=6 a.m. and t_s=6 p.m.

3- Calculation procedure

In numerical calculations, an iterative method is used to bring the effect of the temperature dependence of various heat transfer coefficients. For certain temperatures, they are first calculated by using the standard expressions given earlier. Equations are solved by assuming the constant and the new solutions used to generate all the heat transfer coefficients again till the values converge. The convergence criteria are given the following relationship:

$$\text{Sup}\left[\max_i \left|T_{xi}^{k+1} - T_{xi}^{k}\right|, \left|T_c^{k+1} - T_c^{k}\right|, \left|T_p^{k+1} - T_p^{k}\right|\right] \le \gamma \tag{20}$$

An appropriate choice of the γ is important to make sure that the convergence is rich. Several tests have been made for which, γ tacked 10^{-3}, 10^{-4} and 10^{-5}, the results values and numbers of iterations were compared. The results showed that for the low value of flux ($I(t)<270$ W/m^2), the value $\gamma=10^{-3}$ was satisfactory while, for the higher values of flux I(t), $\gamma\sim 8\ 10^{-4}$ was adequate. The value of γ was kept constant, 10^{-5}, throughout the present calculations. The computer program is based on FORTRAN and proceeds as outlined above.

4- Physical parameters

One collector panel with CPC collectors truncated to one-third of the full size within the acceptance half-angle of 15˚ is considered. The collector has a total aperture area of 0.72 m^2 and a flat plate absorber area of 0.24 m^2. This collector has overall dimensions 0.6 m height, 0.6 m width, 8 mm gap thickness and the calculations are done for three values of CPC length, L, from 1.2 to 2 m. The receiving surface, which is painted non-selective matt black, forms the upper side of a rectangular airflow duct of depth 0.03 m made of aluminium sheet 0.2 mm thick (Pramuang and Exell 2005). The bottom of the duct is insulated with fibre glass 0.05 m thick. The optical properties of the materials in the collector are listed in table 1. The physical properties of air were assumed to vary linearly with temperature within the range encountered in solar air heaters. Therefore, typical linear equations for the viscosity, density, thermal conductivity, and specific heat of air were implemented in the theoretical procedure. The following are recalled in the Appendix. The mean values of the ambient temperature and global radiation in May at Garoua in Cameroon (9°20' N; 13°23' E; altitude 241 m) are used (Tchinda et al. 2004).

5- Results and discussion

A series of runs with individual parameters varied while others, held constant, were conducted and analysed to investigate the influence of these parameters on the thermal performance of the present model. The effect of increasing the volume flow rate on the local air, the air outlet, the absorber plate and the cover temperatures and the instantaneous and daily average efficiencies is presented in figures 2 to 5. It is apparent, as expected, that as the air mass flow rate increases the air flow local temperature and air outlet temperature decreases. Further, for high mass flow rates the collector operating temperature would be lower, resulting in lower heat losses and, subsequently, higher efficiencies. In all the results, it observed is that the absorber plate exhibits the highest temperature, and the cover the

lowest. As air flow rate increases, the temperature differences between the air and the absorber plate decrease. The effects of wind on the instantaneous and daily efficiencies are shown in figure 4-a and b. The results show that by decreasing the value of the wind speed, as expected, the wind heat transfer coefficient decreases, and thus the overall loss coefficient value, instantaneous and daily efficiencies increased.

The effect of increasing the collector length on the thermal performance is displayed in figures 2-a and 5. It can be seen that as the collector length is increased the absorber average temperature is appreciably increased as was the air temperature. However, the instantaneous and daily average efficiencies slightly decrease with the increase in length of the collector, which presumably results from the greater heat losses to the surroundings since both the average absorber temperature and size of the collector are increased. Figure 6 shows the instantaneous efficiency calculated for different solar irradiances.

Figure 7 shows the effect of the air mass flow rate on U_L and F'. It is shown that the collector efficiency factor F' increases with the air mass flow rate. It is also observed, as expected, that U_L decreases with the increase of the air mass flow rate.

Figure 8 compares the efficiency obtained from the present mathematical model and experimental data of Pramuang and Exell (2005). The test data have been taken from a collector having conditions sufficiently close to those given by Pramuang and Exell (2005). It can be seen that the results obtained show a good agreement with experimental data, with an average error of 8%.

6- Conclusion

The heat transfer characteristics and thermal performance of a solar flat plate collector with a CPC has been presented. A theoretical solution procedure of the energy equations using a computer code for predicting the thermal performance of the present solar air heater has been made. The influence of the air mass flow rate, collector length and wind speed on the performance of the present air heater has been discussed. Reasonable agreement is obtained from the comparison between the numerical results and experimental data.

Appendix

The different heat transfer coefficients for each surface in the present system are evaluated as follows.

Radiation heat transfer from the cover to the Sky

The radiative h_{Rp} heat transfer coefficient between the flat plate absorber and the cover is:

$$h_{Rp} = \frac{\sigma\left(T_p^2 + T_c^2\right)\left(T_p + T_c\right)}{\frac{1}{\varepsilon_p} + \frac{A_p}{A_c}\left(\frac{1}{\varepsilon_c} - 1\right)} \tag{A1}$$

Radiation heat transfer from the flat plate absorber to the cover

The radiative heat loss coefficient h_{Rs} between cover and the sky is calculated from the relationship:

$$h_{Rs} = \sigma\ \varepsilon_C (T_C^2 + T_s^2)(T_C + T_s)\frac{A_c}{A_P} \tag{A2-a}$$

where the expression of the sky temperature is given by (Hsieh 1979, Hsieh 1981, Tchinda et al. 1998):

$T_s = T_b - 6$ (A2-b)

Convection heat transfer coefficient from the cover due to wind

The heat loss coefficient by convection $h_{c/a}$ between cover and the ambient is correlated by Duffie and Beckman (1974) as:

$$h_{c/a} = (5.7 + 3.8\ v)\frac{A_c}{A_p} \tag{A3-a}$$

or by Watmuff et al. (1977) as:

$$h_{c/a} = (2.8 + 3.3\ v)\frac{A_c}{A_p} \tag{A3-b}$$

where v is the wind velocity. The Duffie and Beckman correlation was the one that was employed in this study.

Convective heat transfer coefficient between flat plate absorber and cover

According to the Hsieh theory (Hsieh 1981, Tchinda 2003) the convective $h_{p/c}$ heat transfer between the flat plate absorber and the cover is:

$$h_{p/c} = (3.25 + 0.0085 \frac{T_p - T_c}{2\ D_H}) \frac{A_c}{A_P} \quad \text{(A4-a)}$$

where $$D_H = \frac{2\ l_p\ e_f}{l_p + e_f} \quad \text{(A4-b)}$$

The flow is assumed to be hydrodynamically fully developed at the collector inlet. The inner surface convective heat transfer coefficients were modelled according to the flow regime.

- For laminar flow (R_e< 2100) by Mercer correlation (Mercer et al. 1967, Brodkey and Hershey 1988)

$$N_u = 4.9 + \frac{0.0606\ (R_e P_r D_H/L)^{1.2}}{1 + 0.0909\ (R_e P_r D_H/L)^{0.7}\ P_r^{0.17}} \quad \text{(A-4)}$$

- For turbulent flow (R_e>2100) by the Kays correlation presented in a mathematical form by Duffie and Beckman (1980)

$$N_u = 0.0158 R_e^{0.8} \quad \text{(A-5)}$$

With $$R_e = \frac{\dot{m}\ D_H}{l_P\ e_f\ \mu_f}, \quad P_r = \frac{\mu_f C_f}{\lambda_f} \quad \text{(A-6)}$$

Physical properties of air (Ong 1995)

Viscosity: $\mu = [1.983 + 0.00184(T-27)]10^{-5}$ (A-7)

Density: $\rho = 1.1774 - 0.00359(T-27)$ (A-8)

Thermal Conductivity: $\lambda = 0.02624 + 0.0000758(T-27)$ (A-9)

Specific heat: $C_p = 1.0057 + 0.000066(T-27)$ (A-10)

Acknowledgments

This work was done within the framework of the Associateship Scheme of the Abdus Salam International Centre for Theoretical Physics, Trieste, Italy. Financial support from the Swedish International Development Cooperation Agency is acknowledged.

REFERENCES

[1] Adsten M., Hellström B., Karlsson B., Measurement of radiation on the absorber in an asymmetric CPC collector, Solar Energy, 76, pp. 199-206 (2004)

[2} Brodkey R.S. and Hershey H.C., Transport Phenomena, McGraw-Hill Book Company (1988).

[3]] Carvalho M.J., Collares-Pereira M., Gordon J.M. and Rabl A., Truncation of CPC solar collectors and its effect on energy collection, Solar Energy Vol. 35, N° 5, pp. 393-399 (1985)

[4] Duffie J. A. and Beckman W. A., Solar Energy Thermal Processes, Wiley, New York, p.83 (1974)

[5] Duffie J.A. and Beckman W.A., Solar Engineering of Thermal Processes, John Wiley and Sons, New York (1980)

[6]] Eames P.C. and Norton B., Validated, Unified model for optics and heat transfer in line-axis concentrating solar energy collectors. Solar Energy Vol. 50, N°4, pp. 339-355 (1993).

[7] Eames P.C., Smyth M. and Norton B., The experimental validation of a Comprehensive unified model for optics and transfer in line-axis solar energy systems. Solar Energy, 71, pp 121-133 (2001)

[8] Fang, Y. Eames P.C., Hyde T.J. and Norton B., Thermal performance of complex multimaterial frames for evacuated glazing. ISES Solar World Congress, 14th to 19th June 2003, Goteborg, Sweden.

[9] Fraidenraich N., DE R. F. DE Lima, Tiba C. and Barbosa E.M., Simulation model of CPC collector with temperature dependent heat loss coefficient, Solar Energy, Vol. 65, No 2, pp. 99-110, (1999)

[10] Gordon J.M., Ideal solar concentrators for photoelectrochemical cells. Solar Energy Vol. 40, N° 4, pp. 391-395 (1988)

[11] Hsieh C.K., Design of system using CPC collectors to collect solar energy and to produce industrial process steam. Argonne National Laboratory, Rep ANL, pp. 79-102 (1979),

[12] Hsieh C.K., Thermal analysis of CPC collectors, Solar Energy 27,19 (1981)

[13] Mallick T.K., Eames P.C., Hyde T.J. and Norton B., The design and experimental characterisation of an asymmetric compound parabolic photovoltaic concentrator for buiding façade integration in th UK, Solar Energy, 77, pp. 319-327, (2004)

[14] Mercer W.E Pearce. and W.M., Hichcock J.E., Laminar forced convection in the entrance region between parallel flat plates, J. Heat Trans.-T, ASME 89, pp. 251-257, (1967).

[15] Norton B, Prapas D.E., Eames P.C. and Probert S. D., Measured performance of curved inverted-vee, absorber compound parabolic concentrating solar energy collectors. Solar Energy 43, 5, pp. 267-279 (1989)

[16] Ong K.S. Thermal Performance of solar air heaters: Mathematical Model and Solution Procedure, Solar Energy, Vol. 55, 2, pp.93-109 (1995)

[17] Oommen R. and Jayaraman S., Development and performance analysis of compound parabolic solar concentrators with reduced gap losses-oversized reflector, Energy conversion and Management 42, pp. 1379-1399 (2001)

[18] Pramuang S. and Exell R.H.B., Transient test of a solar air heater with a compound parabolic concentrator, Renewable Energy 30, pp. 715-728 (2005).

[19] Prapas D.E., Norton B. and Probert S.D. Thermal design of compound parabolic concentrating solar energy collectors, J. Solar Energy Eng. 109, 161-168 (1987)

[20] Rabl A. Optical and Thermal properties of compound parabolic concentrators. Solar Energy 18, pp. 497-511 (1976)

[21] Rabl A., Goodman N.B. and Winston R., Practical design considerations for CPC

solar collectors, Solar Energy, vol. 22, pp. 373-381 (1979)
[22] Rabl A. and O'Gallagher J. and Winston R., Design and test of non-evacuated solar collector with compound parabolic concentrator, Solar Energy, vol. 25, pp. 335-351 (1980)
[23] Tchinda R.,'Contribution à l'étude des transferts de chaleur dans les systèmes de conversion thermique de l'énergie Solaire: cas des Concentrateurs paraboliques composés' **,**Thèse de Doctorat d'Etat, Université de Yaoundé I, 209 pages (2003)
[24] Tchinda R., Kaptouom E. and Njomo D., Study of the CPC collector thermal behaviour, Energy Convers. Mgmt Vol. 39, N° 13, 1395-1406 (1998)
[25] Tchinda R. and Kaptouom E., Simulation Numérique des Performances d'un Distillateur Solaire Fonctionnant en Mode Indirect, African Journal of sciences and technology pp. 79 – 91 (2004)
[26] Tripanagnostopoulos Y.,Yianoulis P., Papaefthimiou S. and Zafeiratos S., CPC solar collector with bifacial absorbers. Solar Energy 69 (3),pp 191-203 (2000)
[27] Watmuff JH, Carters WWS and Proctor D. Solar and wind induced external coefficients for solar collectors. COMPLESW 2, 56 (1977)

Table 1: The characteristics of the CPCs

Parameter	Symbol	Units	Value
Acceptance half angle	θ_a	°	15
Cover absorptance	$\overline{\alpha}_c$		0.05
Flat plate absorber absorptance	$\overline{\alpha}_p$		0.95
Cover transmittance	$\overline{\tau}_c$		0.89
Cover emittance	ε_c		0.85
Flat plate absorber emittance	ε_p		0.91
Cover reflectance	$\overline{\rho}_c$		0.05
Reflector reflectance	ρ_m		0.86
Flat plate absorber reflectance	$\overline{\rho}_p$		0.15

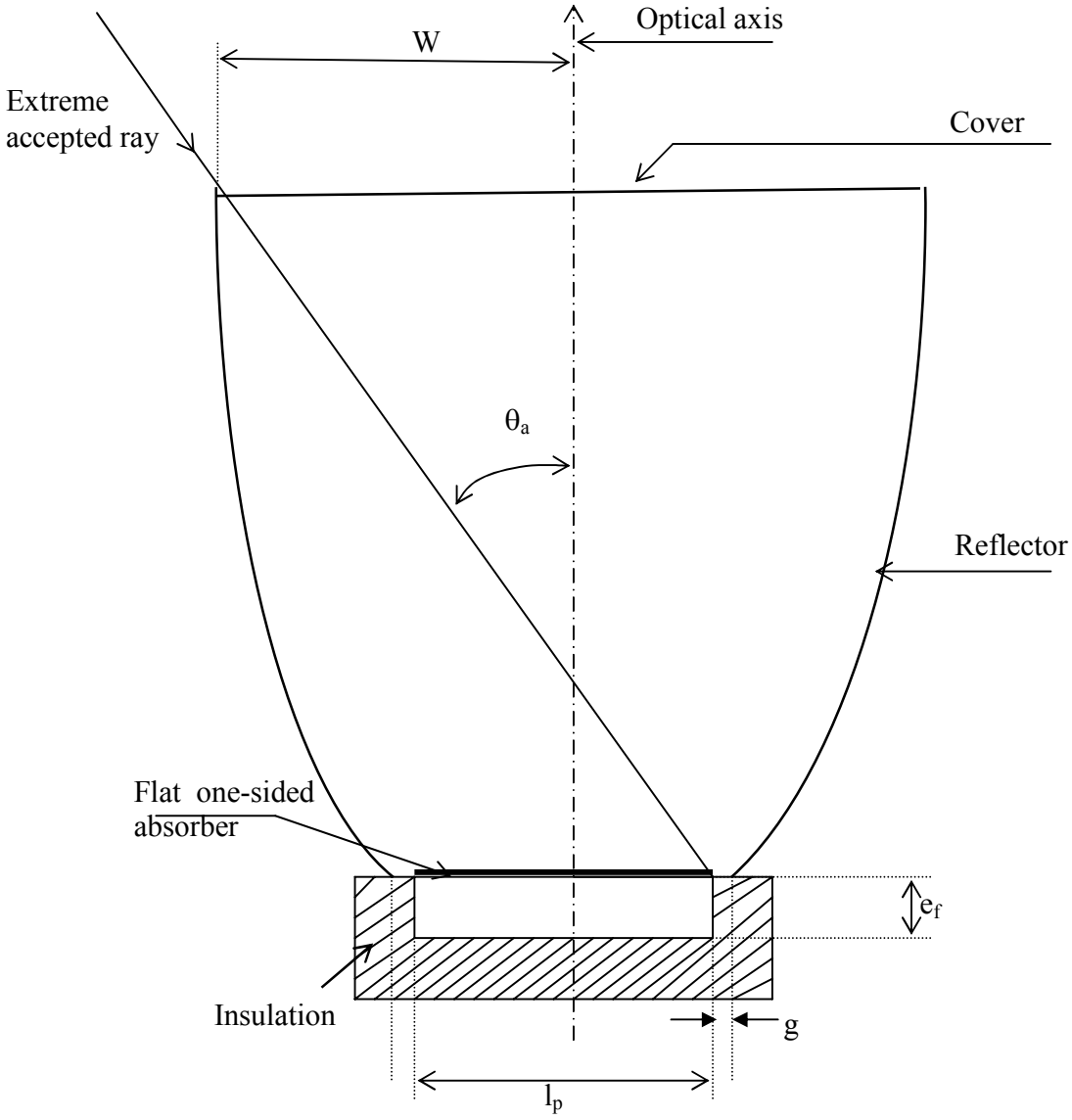

Figure 1: A two-dimensional CPC with a flat one-sided absorber

a- Cross section

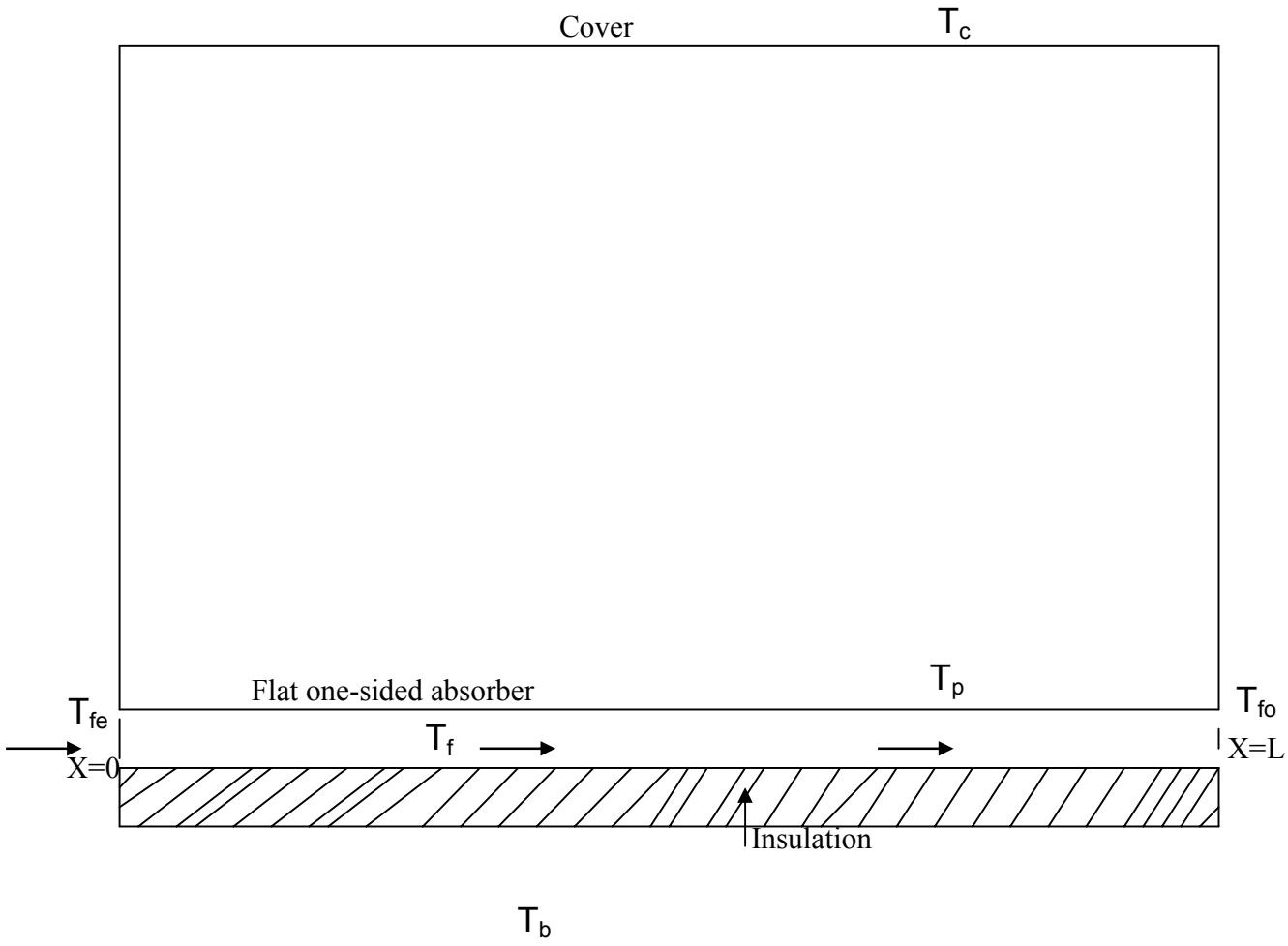

Figure 1: A two-dimensional CPC with a flat one-sided absorber

b- Side view

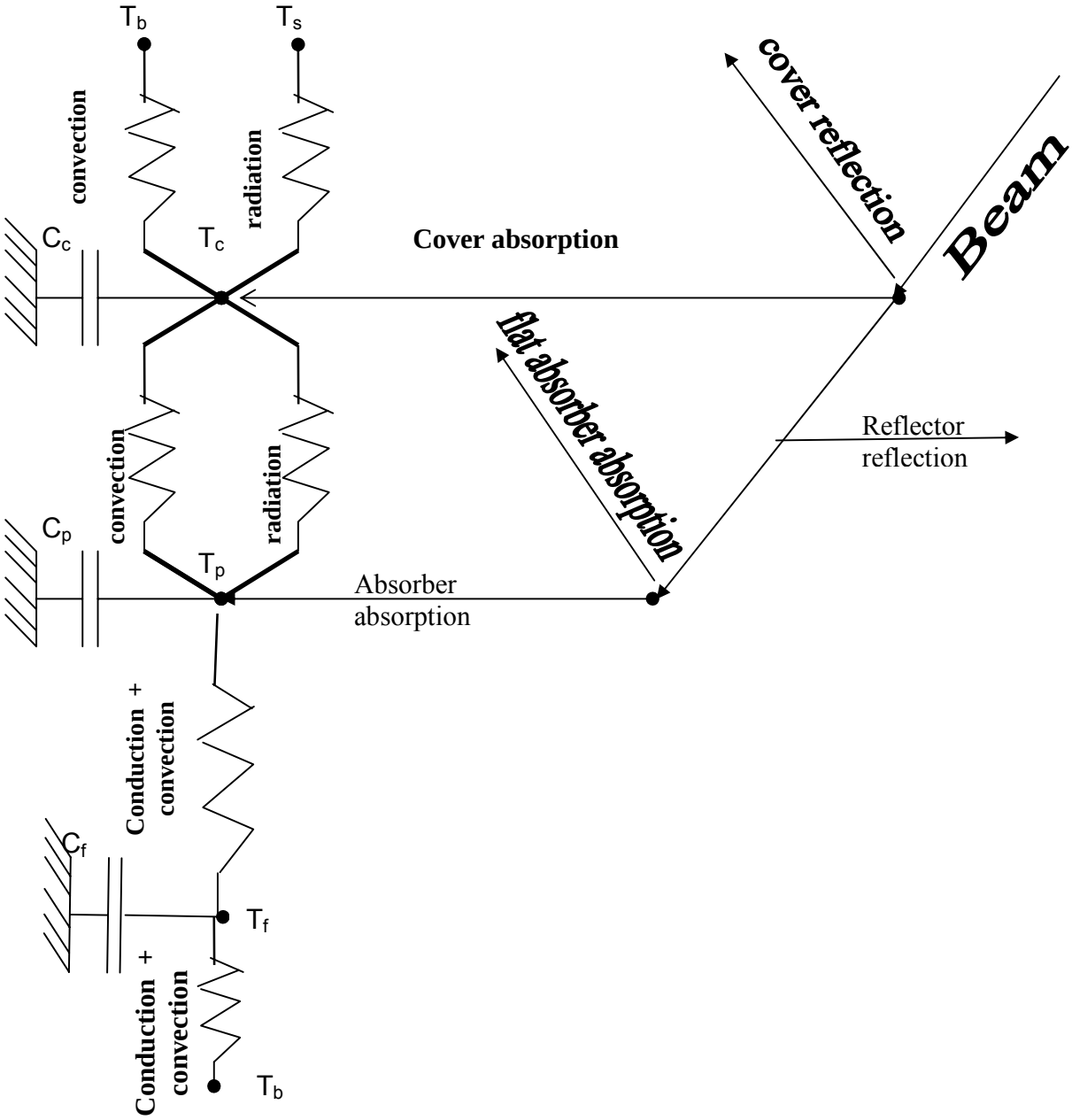

Figure 1: A two-dimensional CPC with a flat one-sided absorber

c: Electric analogy circuit

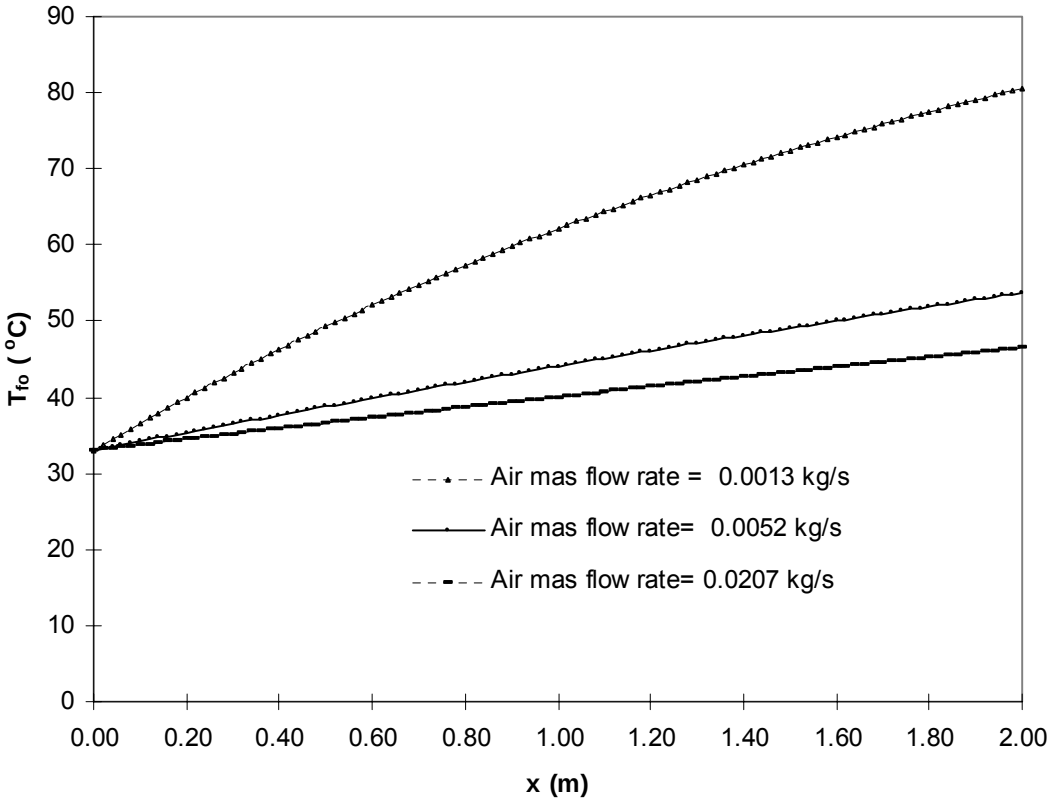

Figure 2-a: Effect of the air mass flow rate on the local temperature in the flow direction; L=1.2m, T_{fe}= 33°C, v=3.0 m/s

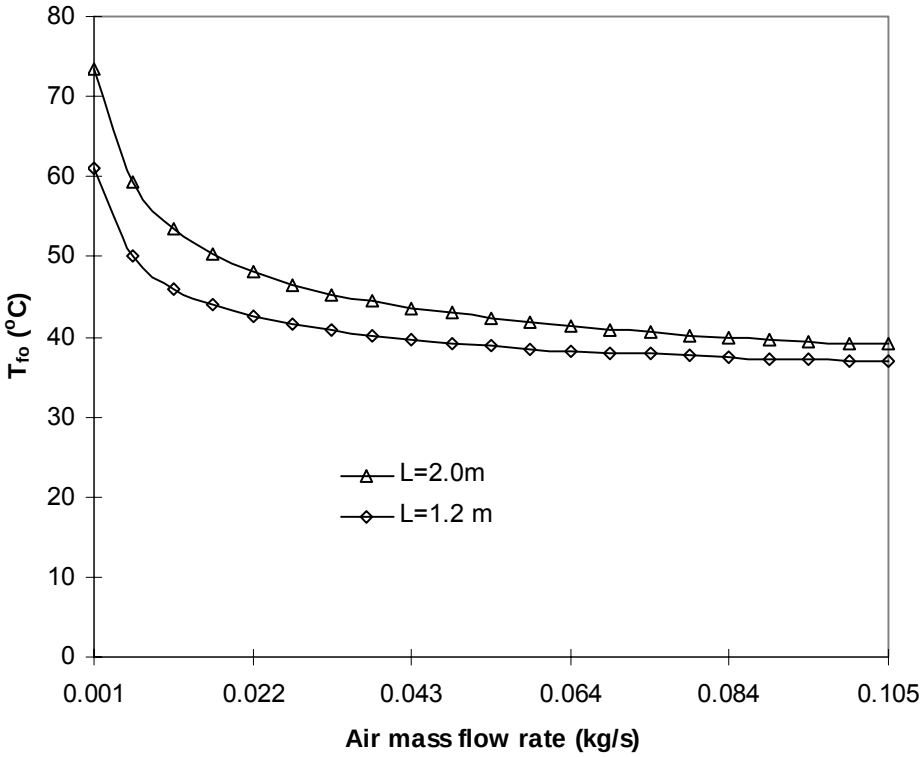

Figure 2-b: The outlet air temperature at t_M=12.30p.m. as a function of the mass flow rate for some values of L

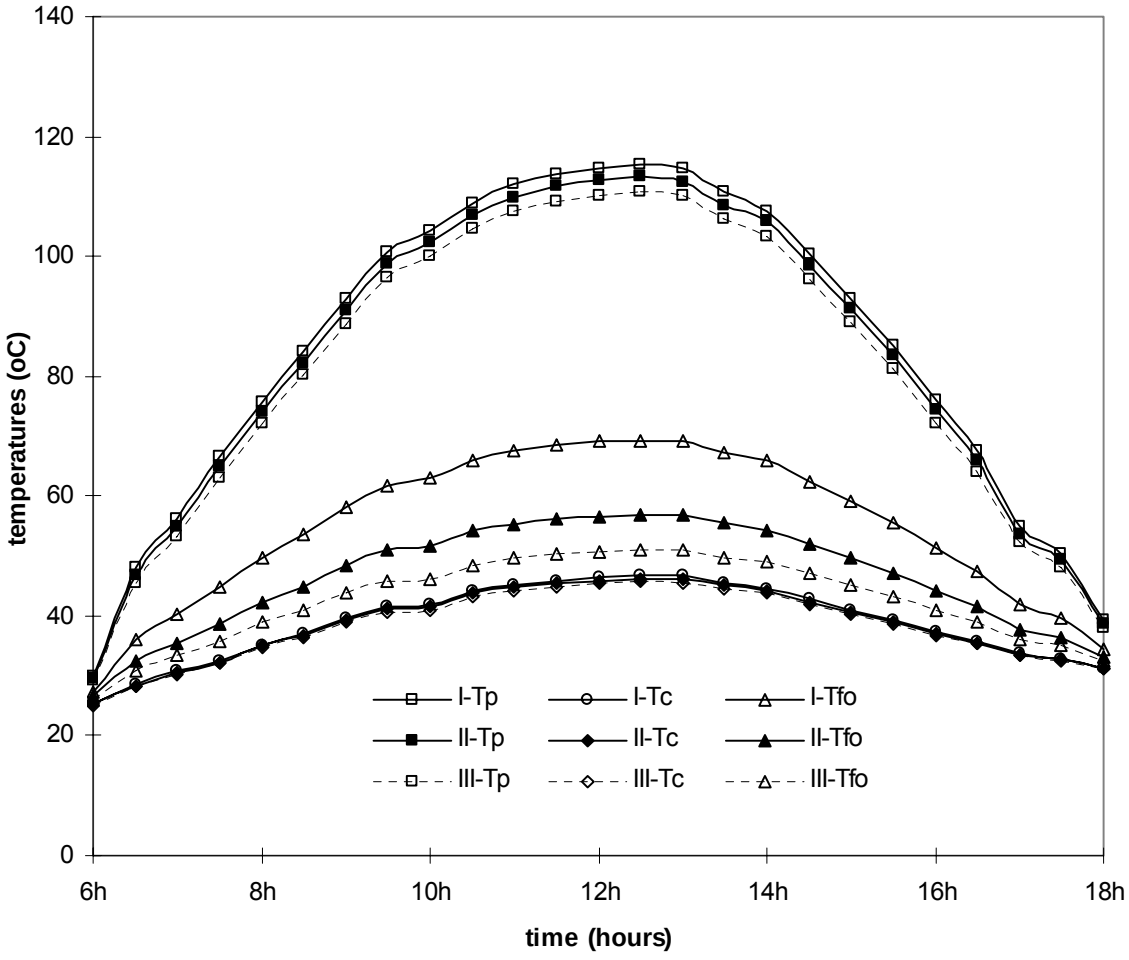

Figure 3: Effect of the air mass flow rate on the hourly variations of temperatures of the collector, **I-** air mass flow rate=0.0013 kg/s; **II-** air mass flow rate=0.0065g/s; **III-** air mass flow rate=0.013 kg/s, L=2.0m

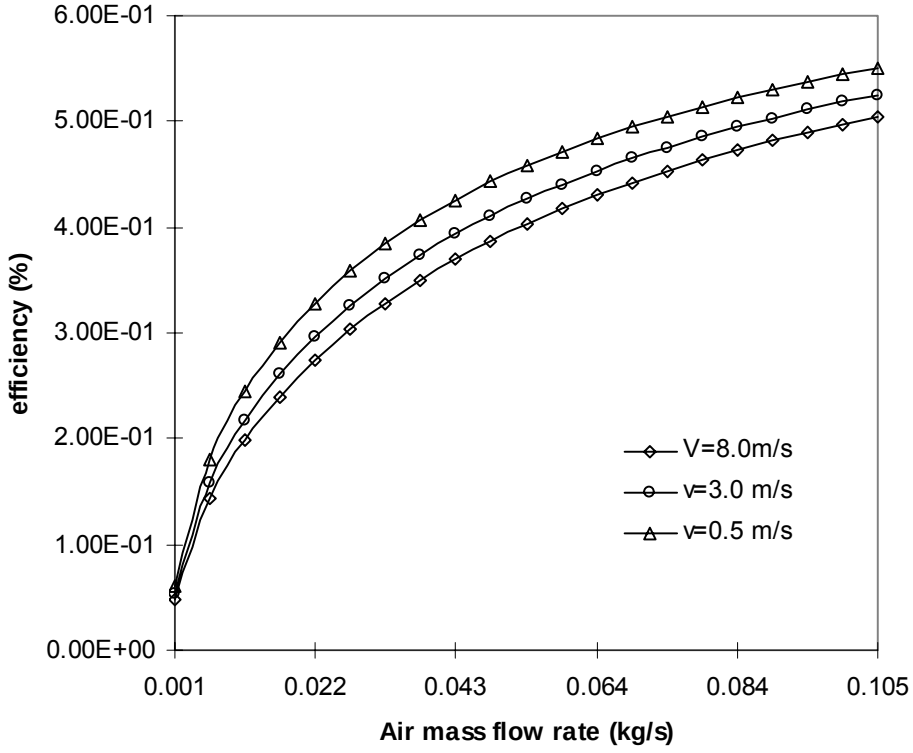

Figure 4-a: Graph of the instantaneous efficiency numerical results for tree wind speeds

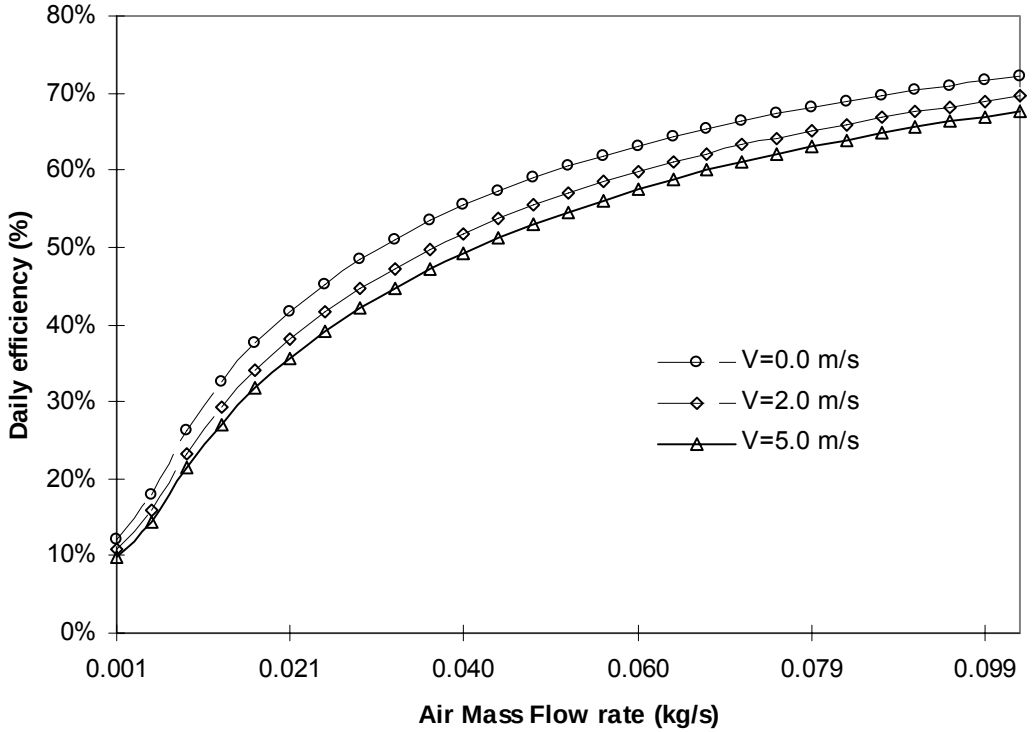

Figure 4-b: Effect of the air mass flow rate on the dailly efficiency for tree values of wind speed, L=1.2 m, T_{fe}=33^{o}C

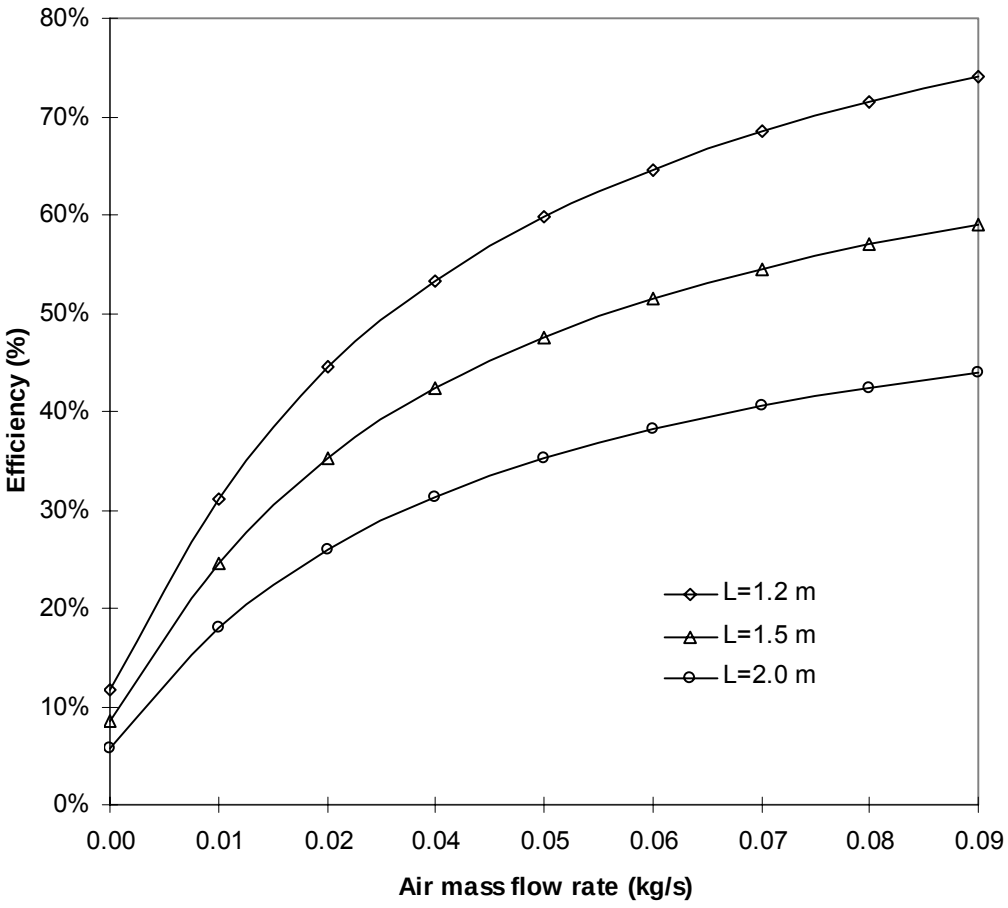

Figure 5-a : Effect of the air mass flow rate on the daily efficiency of the collector for tree values of L

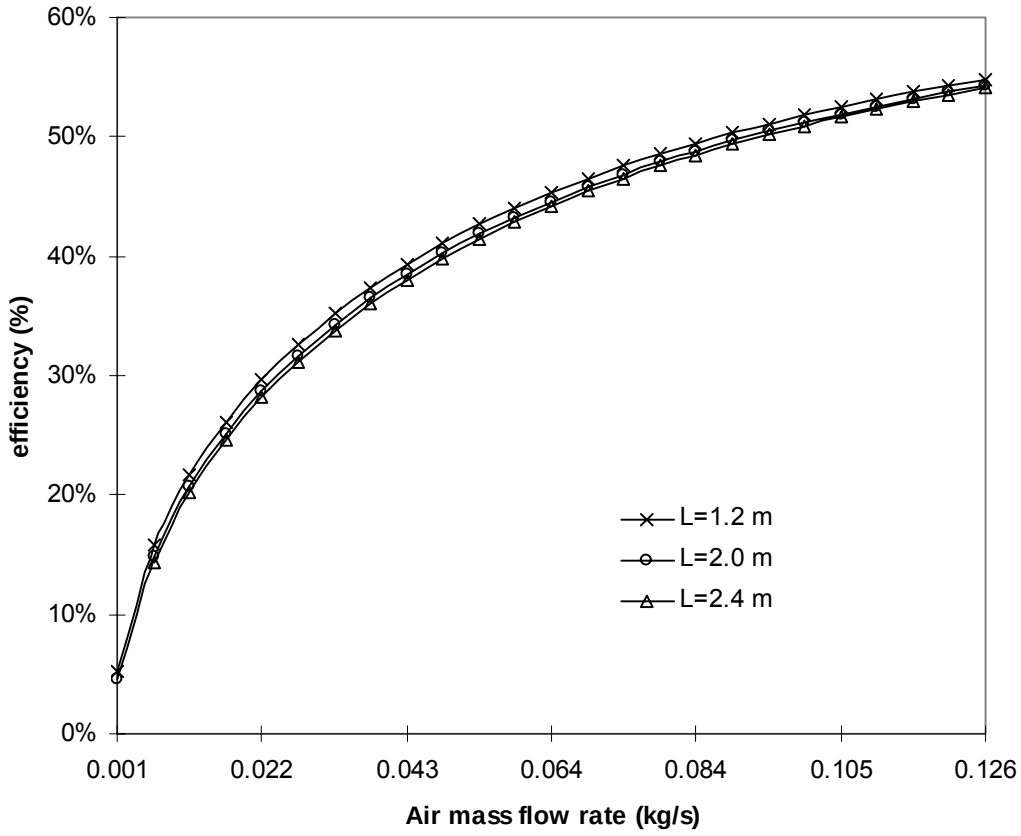

Figure 5-b: Effect of the air mass flow rate and collector length on the instantaneous efficiency at t_M=12.30p.m.

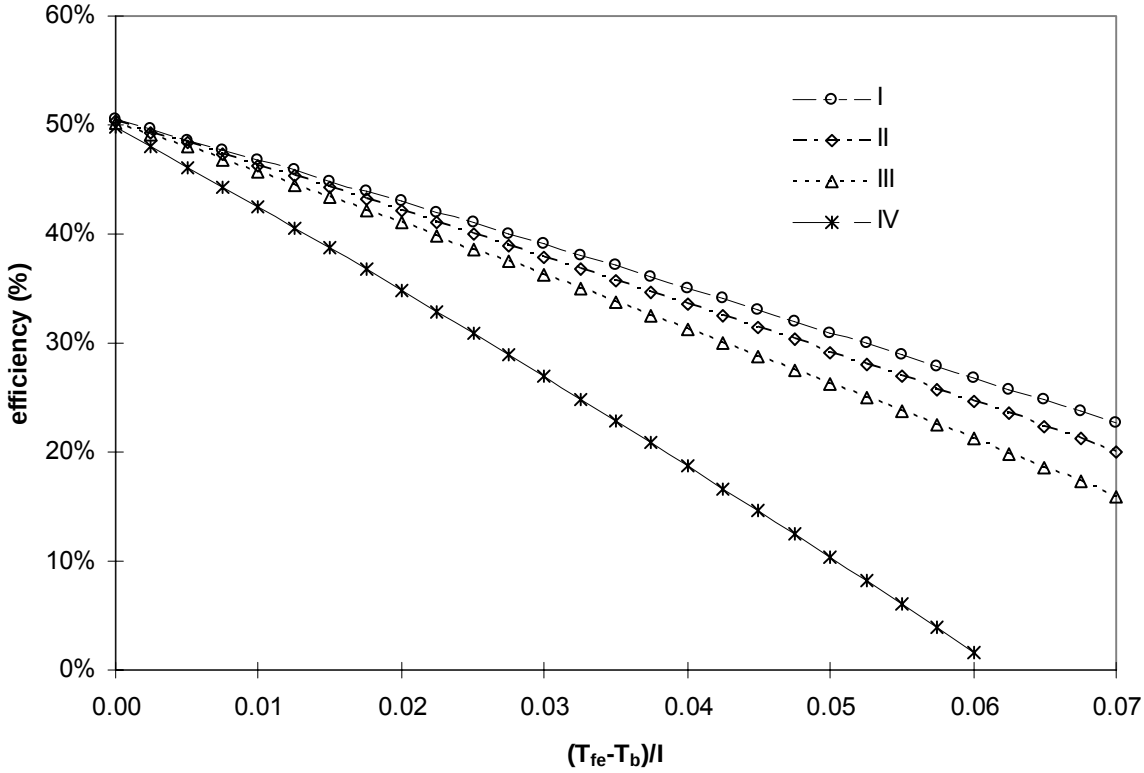

Figure 6: Collector efficiency curves calculated for fourth values of global radiation: I- **I**~951 W/m^2; II- **I**~815 W/m^2; III- **I**~636 W/m^2; IV- **I**~327 W/m^2; v=3,0 m/s, air mass flow rate~0.09 kg/s

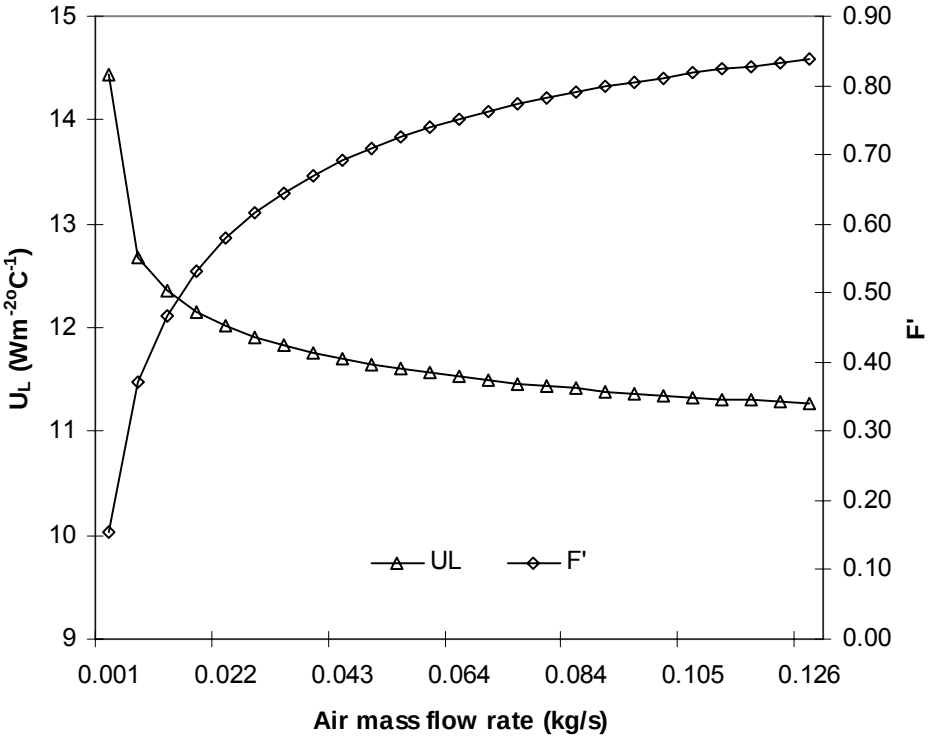

Figure 7: Effect of the air mass flow rate and collector length on F' and U_L

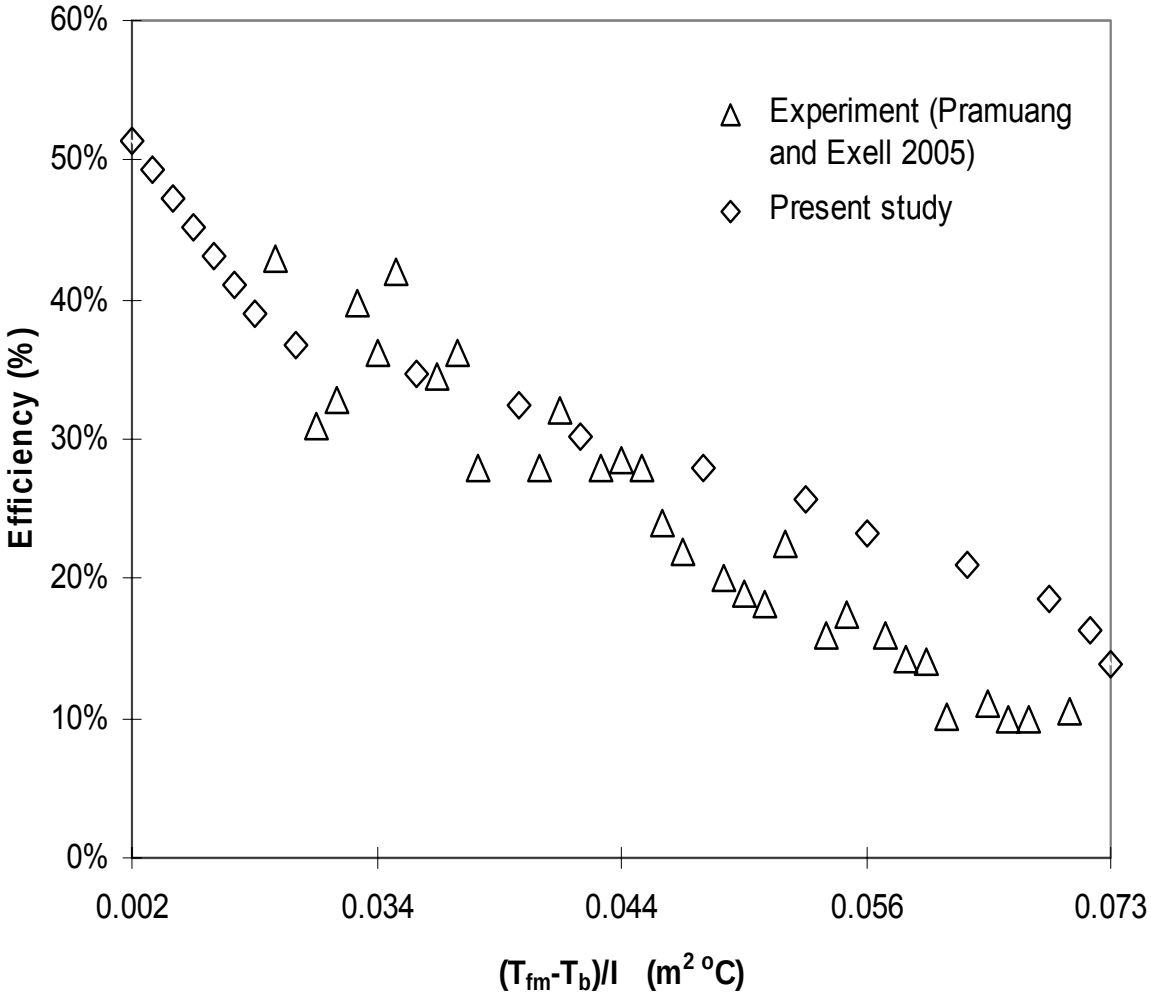

Figure 8: Comparison of the Collector efficiencies